

Growth and Characterization of Pure and Ag⁺ Doped L – Asparagine Monohydrate Single Crystals

P. Kathiravan*¹, S. Sathiskumar², T. Balakrishnan³

¹Crystal Growth Laboratory, PG & Research Department of Physics, Periyar EVR College (Autonomous), Tiruchirappalli – 620023, Tamil Nadu, India.

²Crystal Growth Laboratory, PG & Research Department of Physics, Periyar EVR College (Autonomous), Tiruchirappalli – 620023, Tamil Nadu, India.

³Crystal Growth Laboratory, PG & Research Department of Physics, Periyar EVR College (Autonomous), Tiruchirappalli – 620023, Tamil Nadu, India. balacrystalgrowth@gmail.com

*Corresponding author: balacrystalgrowth@gmail.com

Abstract: Single crystals of pure and Ag⁺ doped L – Asparagine monohydrate (LAM) was successfully grown by slow evaporation method at room temperature. Grown crystals were characterized by single crystal and powder X-ray diffraction analysis. The presence of various functional groups were identified from FTIR spectral analysis. The incorporation of Ag⁺ into the crystal was confirmed from energy dispersive X-ray spectroscopy (EDS). UV – Vis – NIR spectral analysis, Dielectric and Vickers microhardness test were studied. Crystal defects and surface morphology was revealed for both pure and doped crystals from etching studies.

Keywords: Crystal growth, X-Diffraction, UV – Vis – NIR spectrum, Microhardness, Dielectric studies.

1. Introduction

Amino acids are the molecular building blocks of peptides and proteins. L-Asparagine monohydrate (LAM) is an interesting material from amino acid family to investigate because it crystallizes in a structure exhibiting a complex network of hydrogen bonds among asparagine molecules and between asparagine and water molecules [1]. Verbist et al., have reported that L - Asparagine monohydrate (LAM) single crystal crystallizes in orthorhombic structure [2] and belong to space group P2₁2₁2₁ with four molecules per unit cell. Its lattice parameters are $a = 5.597 \text{ \AA}$, $b = 9.819 \text{ \AA}$, $c = 11.792 \text{ \AA}$ and $V = 648.05 \text{ \AA}^3$. Recently, investigation of Mn²⁺ doped L - asparagine monohydrate single crystal has been found to improve the crystallinity, optical transparency and mechanical strength that are useful for optoelectronic application as reported by Mohd.Shakir *et al.*, [3]. Several researchers have carried out organic and metal ion-doped crystal growth and characterization of LAM crystals [4 - 7]. Present, work deals with the growth, structural, optical, thermal, mechanical, dielectric and etching of pure and Ag⁺ - doped LAM single crystals grown by slow evaporation method.

2. Experimental

2.1 Crystal Growth

Saturated solution of pure LAM and 1 mol% of AgNO₃ doped LAM was prepared separately temperature. Both the solution were stirred continuously for about three hours using the magnetic stirrer and filtered using whatman filter paper. Filtered solution was covered with perforated polythene sheet and kept for crystallization. Good quality pure LAM single crystal of size 18 × 14 × 6 mm³ was harvested after a

growth period of 11 days is shown in Fig.1(a). Ag⁺ doped LAM single crystal of size 10 × 5 × 4 mm³ was harvested after the growth period of seven days is shown Fig.1(b).

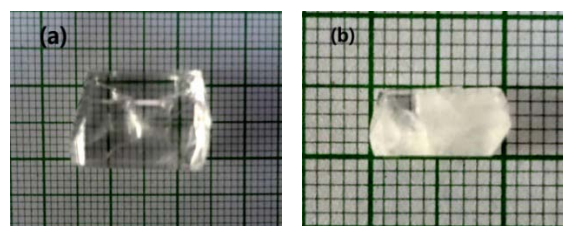


Figure 1(a): As grown Pure LAM and (b): Ag⁺ - doped LAM crystals

3. Result And Discussion

3.1 Single Crystal X – Ray Diffraction

In order to identify the lattice parameters of the grown crystals, single crystal X – ray diffraction study was performed by using ENRAF – NONIUS CAD 4 diffractometer with CuK α radiation source ($\lambda = 1.5404 \text{ \AA}$). The single crystal XRD data shows that both pure and Ag⁺ doped LAM crystals belongs to orthorhombic system with non-centrosymmetric space group P2₁2₁2₁. The lattice parameters of LAM crystals are in good agreement with the reported values[2]. The estimated lattice parameter values of the pure and Ag⁺-doped LAM crystals were compared and is presented in Table 1. A marginal decrease in the lattice parameters and volume has been observed for the Ag⁺-doped LAM crystal in comparison with the pure LAM crystal.

Table - 1 Single Crystal X – Ray Diffraction Data Of Pure And Ag⁺ – Doped Lam Crystals

Cell Parameters	Pure LAM	Ag ⁺ -doped LAM
a	5.593 (Å)	5.604 (Å)

UGC Sponsored National Conference on

Advanced Technology Oriented Materials (ATOM-2014), 8-9th Dec-2014

Department of Physics, Government College (A), Rajahmundry, Andhra Pradesh, India

b	9.827 (Å)	9.841(Å)
c	11.808 (Å)	11.8792 (Å)
α	90°	90°
β	90°	90°
γ	90°	90°
V	648.996 Å ³	654.05 Å ³
Crystal system	Orthorhombic	Orthorhombic
Space group	P2 ₁ 2 ₁ 2 ₁	P2 ₁ 2 ₁ 2 ₁

3.2 Powder X – Ray Diffraction Analysis

As-grown pure and Ag⁺-doped LAM crystals were finely powdered and subjected to powder XRD analysis using the Rich Seifert diffractometer. The samples were examined with CuK α radiation in a 2 θ range of 10 - 80° at a scan rate of 0.5°/ minute. The powder XRD patterns of Ag⁺ - doped samples are compared with that of undoped one Fig. 2. However, a slight variation in intensity is observed as a result of doping. The most prominent peaks with maximum intensity of the XRD patterns of pure and doped specimens are quite different.

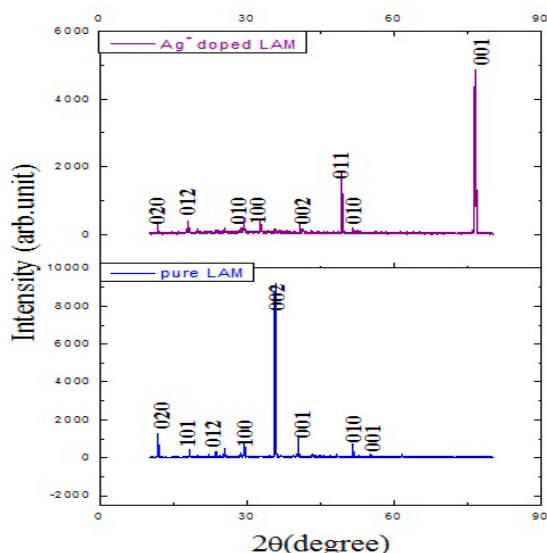


Figure 2: Powder X - ray diffraction pattern of pure and Ag⁺-doped LAM crystal

3.3 FT - IR Analysis

The FT - IR spectrum of pure and Ag⁺-doped LAM crystals were recorded on Perkin - Elmer FTIR spectrometer using KBr pellet technique in the range of 4000 - 400 cm⁻¹ are shown in Figure 3. A peak appeared at 3781 cm⁻¹ indicating the presence of O - H stretching vibration. The intense and fairly sharp band at 3383 cm⁻¹ is assigned to the NH₂ asymmetric stretching vibration. The appearance of the broad band at 3110 cm⁻¹ is due to the NH₃ symmetric stretching vibration confirming the zwitter ion structure of the molecule. The N - H symmetric stretching vibration is observed in 2745 cm⁻¹. The band at 2000 - 2148 cm⁻¹ is attributed to NH₃ deformation vibration in FT - IR spectrum [8]. The peaks occur at 1769 cm⁻¹ is due to symmetric stretching vibrations of C = O. Other characteristic vibrations establishing the identity of the functional groups present in the compounds are represented in Table.2. Although the spectrum of Ag⁺-doped LAM provides similar features as

that of pure LAM, there is slight shifting observed suggesting that it may be due to the incorporation of Ag⁺ ions in the lattice of LAM. Analysis of the surface at different sites reveals that the incorporation of Ag⁺ is non-uniform over the host crystal surface.

TABLE - 2 : FTIR Spectral Assignments Of Pure And Ag⁺ - Doped Lam Crystals.

Pure LAM (cm ⁻¹)	Ag ⁺ -doped LAM (cm ⁻¹)	Band assignments
3781	3781	O-H ν
3382	3383	NH ₂ ν
3110	3113	NH ₃ ⁺ ν
2948	2946	NH ₃ ⁺ ν
2745	2755	NH S ν_s
2148	2149	N - H ν
2000	2001	N - H ν
1769	1758	C = O ν
1358	1359	CH ϕ
1232	1234	NH ₂ ρ
1148	1130	NH ₃ ⁺ ρ
836	835	C - C ν

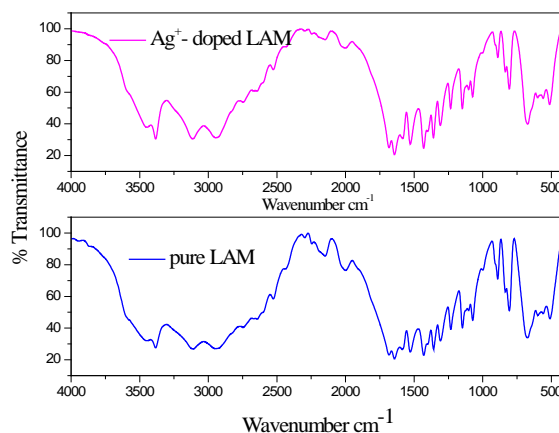


Figure3: FTIR spectrum of pure LAM and Ag⁺ doped LAM crystals.

3.4 Edax Studies

Energy Dispersive X - rays Analysis (EDAX) is a technique used for identifying the elemental composition of the specimen. In this study, the grown crystals were analyzed by FEI QUANTA 200F energy dispersive X - ray microanalyzer. The incorporation of Ag⁺ in the doped specimen was confirmed by EDS qualitative analysis as clearly seen in Fig.4. The weight percentage (wt%) of C, O, N and Ag as obtained from EDAX analysis for Ag⁺-doped LAM crystals are and presented in Table 3. From the experimental data, the presence of Ag⁺ crystal is confirmed.

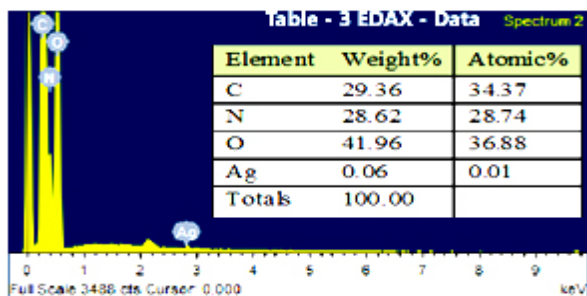


Figure 4: EDAX Spectra of pure and Ag^+ -doped LAM crystals

3.5 UV – Vis – Nir Spectral Studies

UV – Vis – NIR transmittance Spectrum of pure and Ag^+ -doped LAM single crystal of thickness 2 mm was used to record the spectrum in the wavelength range 200 - 1100 nm using Lambda 35 UV – Vis – NIR spectrophotometer. A nonlinear optical material can be used for practical application only if it has a wide transparency window. Fig.5(a) shows the transmittance spectrum of pure and Ag^+ -doped LAM single crystals. The lower cut-off wavelength occurs at 196 nm and 194 nm for pure and Ag^+ -doped LAM respectively. Absorption in the near ultraviolet region arises from electronic transitions associated within the sample.

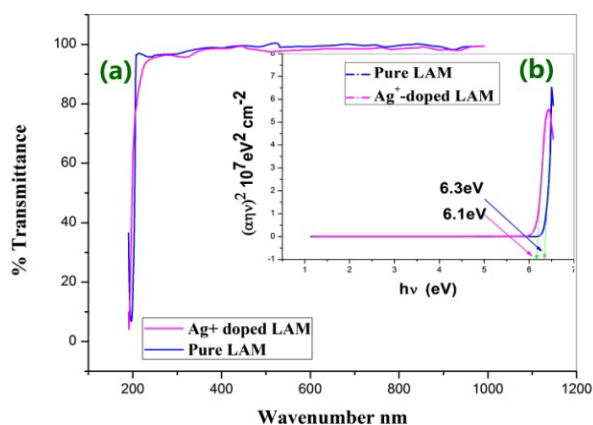


Figure 5: (a) UV – Vis - NIR transmittance spectrum and (b) Plot of $(\alpha hv)^2$ versus $h\nu$ of pure and Ag^+ -doped LAM crystals.

The optical absorption coefficient (α) was calculated from the transmittance spectrum using the following relation, $\alpha = 1/t \log(1/T)$ where, T is the transmittance and t is the thickness of the crystal. The direct optical band determined using the relation $\alpha = A(h\nu - E_g)^{1/2}/(h\nu)$ where, E_g is optical band gap energy of the crystal and A is a constant. The plot of $(\alpha hv)^2$ versus $h\nu$ is shown in Figure 5(b). E_g is evaluated by the extrapolation of the linear part of the graph. The calculated band gap energy is found to be 6.3 eV for pure LAM and Ag^+ -doped LAM is 6.1 eV.

3.6 Dielectric Studies

The dielectric study of pure and Ag^+ -doped LAM single crystals were carried out using the instrument HIOKI 3532 - 50 LCR HITESTER. A sample of dimension $4 \times 2 \times 2 \text{ mm}^3$

having graphite coating on the opposite faces was placed between the two copper electrodes and thus a parallel plate capacitor was formed. The capacitance of the sample was measured by varying the frequency from 50 Hz to 200 KHz at room temperature. The dielectric constant was calculated using the formula $\epsilon_r = (Ct)/(\epsilon_0 A)$, where C is capacitance (Farads), t the thickness (m), A the area (m^2), ϵ_0 is the absolute permittivity in the free space. Fig.7 Shows the variation of the dielectric constant (ϵ_r) with applied frequency. The value of dielectric constant is high in the lower frequency region and then it decreases with increase of frequency.

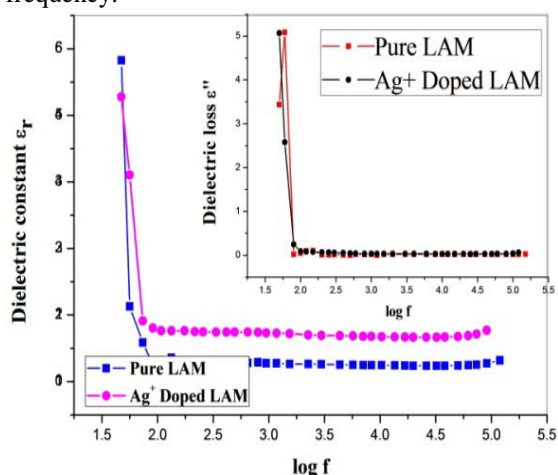


Figure 7: Dielectric constant & Dielectric loss of a pure and Ag^+ -doped LAM crystals.

The high value of dielectric constant at low frequencies may be due to the presence of all the four polarizations and its low value at high frequencies may be due to the loss of significance of these polarizations gradually [9]. Similarly, the dielectric loss was calculated using the relation $\epsilon'' = \epsilon_r \tan \delta$. The variation of dielectric loss with frequency is shown in Fig. 7. In the case of Ag^+ -doped LAM, the same trend is observed with reference to pure LAM. However it is marginally altered in the dielectric behaviour of pure LAM, which may be due to the incorporation Ag^+ metal ion dopant.

3.7 Vicker's Microhardness Studies

Hardness is the resistance offered by a material against the plastic deformation caused by scratching or indentation. The Vickers microhardness measurements were carried out on pure and Ag^+ -doped LAM crystal using SHIMADZU HMV - 2000 microhardness tester. The static indentation were made at room temperature with a constant indentation time 3s. The diagonal impressions of the indentation marks made on the surface by varying load from 25g to 100g were measured. The Vicker's hardness (H_v) numbers at different loads were calculated using the following relation, $H_v = 1.8544/d^2(\text{kg}/\text{mm}^2)$ where P is applied load in kg, 1.8544 is a count of a geometrical factor for the diamond pyramidal indenter and d is the average diagonal length of the indenter impression in mm.

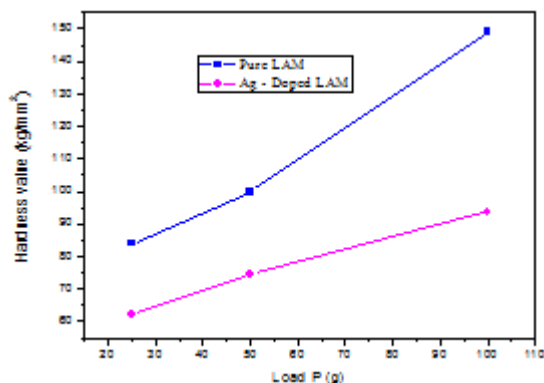


Figure 9: Microhardness behaviour of pure and Ag⁺-doped LAM crystals.

The value of hardness increases with increase in applied load and above 100 g cracks were developed around the indentation mark for pure and doped LAM due to the release of internal stress generated locally by indentation. From the results, it is observed that the value of hardness of the pure LAM crystal is higher than the hardness value of Ag⁺-doped LAM single crystals for all loads. This decrease in the hardness value of doped sample can be attributed to the incorporation of the impurity in the lattice of the LAM crystal is shown in Fig. 9.

3.8 Etching Analysis

The Chemical Etching studies were carried out on the grown crystals of pure LAM and Ag⁺-doped LAM using polarized high resolution optical microscope to study the symmetry of the crystal face from the shape of etch pits and distribution of structural defect in the grown crystals. The surface of the crystal was polished finely before the etching process. The crystal was dipped 10s in water etchant for etching. The etch patterns recorded using motic camera are presented in the Figure 11(a) and (b). The shape of the etch pits may be changed by varying the amount of the solvent. The etch patterns obtained also depend upon the nature of the etchant.

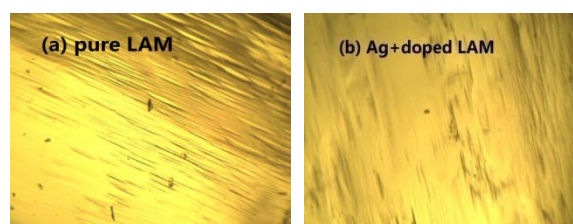


Figure 11: Etch patterns of (a) pure LAM and (b) Ag⁺-doped LAM crystals for.

4. CONCLUSION

The single crystals of pure and Ag⁺ doped L - Asparagine monohydrate single crystals were grown from aqueous solution by slow evaporation technique at room temperature. Single crystal X - ray diffraction studies confirm that both pure and Ag⁺-doped LAM crystals crystallize in orthorhombic crystal system. The UV cut - off wavelength of pure LAM and Ag⁺-doped LAM is observed at 196 nm and 194 nm respectively. The FTIR spectrum confirms the presence of functional groups of the grown single crystals.

The incorporation of Ag⁺ metal ion in the LAM crystal is confirmed by EDAX spectral analysis. The dielectric studies reveals that the value of dielectric constant and dielectric loss of the crystal is low at high frequency region. The value of microhardness increases with the increase of applied load for both pure and Ag⁺ doped LAM single crystals. It is interesting to note that the incorporation of dopant have slightly decreased the hardness of the parent. Etch patterns of grown Ag⁺-doped LAM crystal shows the crystalline perfection.

Reference

- [1] M.Ramanadham, S.K.Sikka, and R.hidambaram, "Structure of L - asparagine monohydrate by neutron diffraction" IUCR, Acta Crystallography. B28(10), pp.3006–3005, 1972.
- [2] J.J.Verbist, M.S.Lehman, T.F.Koetzla, and W.C.Hamilton, The "Crystal and Molecular Structure of the Amino Acid L-Asparagine Monohydrate" Acta Crystallography, IUCR, B 28(10), pp.3006–3013, 1972.
- [3] Mohd. Shakir, V.Ganesh, M.A.Wahab, G. Bhagavannarayana, and K.Kishan Rao, "Structural, optical and mechanical studies on pure and Mn²⁺ doped L-asparagine monohydrate single crystals" Materials Science and Engineering B, ELSEVIER, pp.172 9-14, 2010.
- [4] K.Krambrock, K.J.Guedes, L.O. Ladeira, M.J.B. ezerra, T.M.Oliveira, G.A.Bezerra, Cavada, M.C.F., B.S.de Oliveria, M.Z.S.Flores, G.A.Farias, and V.N.Freire, "Inhomogeneous, disordered, and partially ordered systems-Two different incorporation sites of manganese in single-crystalline monohydrated L-asparagine studied by electron paramagnetic resonance" Physical Review-Section B-Condensed Matter, AIP, 75(10), PP.104205-104205, 2007.
- [5] K.Moovendaran, R.Bikshandarkoil Srinivasan, J. Kalyana Sundar. S.A.Martin Britto Dhas , and S.Natarajan, "Structural, vibrational and thermal studies of a new nonlinear optical material: L-asparagine-L-tartaric acid". Spectrochimica Acta Part A, ELSEVIER 92, PP. 388 – 391, 2012.
- [6] N.Peeresy, M.Souhassouyx, B. Wynckey, G. Avoilleyx, and A.Coussonzand, "Neutron diffraction study of the paraelectric phase of ammonium dihydrogen phosphate (ADP): hydrogen bonding of NH⁴⁺". Journal of Physics: Condensed Matter, IOP SCIENCE, 9(10), PP.6555, 1997.
- [7] R.Reintjes, and E.C. Eckardt, "Efficient harmonic generation from 532 to 266 nm in ADP and KDP" Applied Physics Letters, AIP 30(10), 91, 1997.
- [8] K.Nakamoto, Infrared and Raman Spectra of Inorganic and Coordination Compounds, John Wiley and Sons, New York, 1978.
- [10] [9] R.Uthrakumar, C. Vesta, R. Robert, G. Mangalam and S.Jerome Das, "Optical and mechanical studies on unidirectional grown tri-nitrophenol methyl p-hydroxybenzoate bulk single crystal" Physica B, ELSEVIER, 405(10), PP.4274-4278, 2010.